

# Meridional Flow, Differential Rotation, and the Solar Dynamo

Manfred Küker<sup>1</sup>

<sup>1</sup>*Leibniz Institut für Astrophysik Potsdam, An der Sternwarte 16, 14482 Potsdam, Germany*

**Abstract.** Mean field models of rotating convection zones reproduce the solar differential rotation remarkably well. We discuss the effects of Reynold stress and baroclinity on the meridional flow and the implications for stellar dynamo models. As it turns out the Reynolds stress is required to reproduce both the internal rotation pattern observed by helioseismology and the flow pattern required by the flux transport dynamo.

## 1. Introduction

While it is widely accepted that the solar activity cycle is the result of a dynamo mechanism involving differential rotation and helicity, there is no consensus about the detailed mechanism. The  $\alpha\Omega$  dynamo is an interplay of the differential rotation and the kinetic helicity of the convective motions in the rotating, stratified convection zone. The differential rotation will wind up the poloidal field and thus (re)generate the toroidal field. The kinetic helicity ( $\alpha$  effect) generates a (usually weak) poloidal field from an existing toroidal field. Together, the two can generate a strong large-scale field from an arbitrarily weak initial seed field.

Helioseismology does not confirm the assumption made in older models that the rotation rate increases with depth through the whole convection zone. Instead, the radial shear is weak in the bulk of the convection zone. A pronounced depth-dependence of the rotation rate is found only in the super granulation layer, where  $\partial\Omega/\partial r < 0$  and in the transition layer at the bottom of the convection zone, where the shear is positive at low and negative at high latitudes (Thompson et al. 2003). Models were therefore constructed that used the positive shear at low latitudes at the bottom of the convection zone and the negative  $\alpha$  effect resulting from positive helicity (in the northern hemisphere) of the overshooting convection to form an  $\alpha\omega$  dynamo at the bottom of the convection zone. This overshoot dynamo has, however, produces a rather complicated field geometry a cycle time much shorter than the observed 11 years (cf. Rüdiger & Brandenburg 1995).

A possible solution is the flux transport dynamo (Choudhuri et al. 1995), which uses the large-scale meridional flow to connect the positive helicity in the upper part of the convection zone with the shear layer at the bottom. In this scenario, the cycle period is largely determined by the meridional flow speed and not an intrinsic property of the solution to the dynamo equations ("dynamo waves"). Unfortunately, the meridional flow in the solar interior is not well known. While flows of 10-20 m/s away from the equator have been observed for some time in the surface layer (Komm et al. 2013), the flows at greater depths are still uncertain. Fortunately, the mean field theory used to construct dynamo models can also make predictions for the meridional flow.

## 2. Mean field models of stellar rotation

The equation of motion for the large-scale (mean) gas flow in the convection zone is the Reynolds equation,

$$\rho(\bar{\mathbf{u}} \cdot \nabla)\bar{\mathbf{u}} = -\nabla \cdot \rho\mathbf{Q} - \nabla P + \rho\mathbf{g} \quad (1)$$

where  $\rho$  is the mass density,  $\bar{\mathbf{u}}$  the mean gas velocity,  $P$  the pressure,  $\mathbf{g}$  gravity, and  $Q_{ij} = \langle u'_i u'_j \rangle$  is the one point correlation tensor of the velocity fluctuations.  $\mathbf{Q}$  is related to the Reynolds stress  $\mathcal{R}$  through  $\mathcal{R}_{ij} = -\rho Q_{ij}$ . In the axisymmetric case, the Reynolds equation can be reduced to a system of two scalar equations. The azimuthal component of Equation 1,

$$\nabla \cdot \mathbf{t} = 0, \quad (2)$$

where the angular momentum flux vector  $\mathbf{t}$  is defined through

$$t_i r \sin \theta (\rho r \sin \theta \Omega u_i^m + \rho Q_{i\phi}), \quad (3)$$

expresses the conservation of angular momentum. The meridional flow is governed by the azimuthal component of the curl of the Reynolds equation,

$$\left[ \nabla \times \frac{1}{\rho} \nabla \cdot \mathcal{R} \right]_{\phi} + r \sin \theta \frac{\partial \Omega^2}{\partial z} + \frac{1}{\rho^2} (\nabla \rho \times \nabla p)_{\phi} + \dots = 0, \quad (4)$$

where  $\mathbf{R}$  the Reynolds stress,  $\Omega$  the angular velocity,  $\partial/\partial z = \cos \theta \partial/\partial r - \sin \theta \partial/\partial \theta$  the derivative in the direction parallel to the rotation axis, and  $p$  the pressure. The dots indicate higher order terms that can be neglected in this context. The last term on the left hand side expresses the baroclinicity of the convection zone, i.e. the circumstance that in a rotating convection zone the gradients of density and pressure are not perfectly aligned. For sufficiently large values of the Taylor number,  $\text{Ta} = (4\Omega^2 R_{\star}^4 / \nu_{\text{T}}^2)$ , where  $\nu_{\text{T}}$  is the turbulence viscosity and  $R_{\star}$  the stellar radius, the Reynolds stress is negligible and the meridional flow is the result of the balance between the differential :

$$\frac{\partial \Omega^2}{\partial z} + r \sin \theta \frac{\partial s}{\partial \theta} \approx 0, \quad (5)$$

where the baroclinic term has been expressed in terms of a horizontal derivative of the specific entropy. In case of an isothermal gas Equation 5 reduces to  $\partial \Omega^2 / \partial z \approx 0$ . If Eq. 5 is fulfilled the gas is said to be in thermal wind equilibrium. In this case the thermal

structure determines the rotation pattern and the meridional flow vanishes. The thermal wind equilibrium can generally not be fulfilled near the boundaries, though, as the rotation pattern it produces is not stress-free.

Current mean field models of stellar rotation (e.g. Küker et al. 2011) also include the equation of convective heat transport,

$$\nabla \cdot (\mathbf{F}^{\text{conv}} + \mathbf{F}^{\text{rad}}) - \rho T \bar{\mathbf{u}} \cdot \nabla s = 0, \quad (6)$$

where  $\mathbf{F}^{\text{conv}}$  and  $\mathbf{F}^{\text{rad}}$  are the convective and radiative heat fluxes and  $T$  the gas temperature.

To complete the system formed by equations 1, 4, and 6, expressions for the turbulent transport terms are needed. The second order correlation approximation allows it to express the Reynolds stress and the convective heat flux in terms of mean quantities:

$$Q_{ij} = -\mathcal{N}_{ijkl} \frac{\partial \bar{u}_l}{\partial x_k} + \Lambda_{ijk} \Omega_k, \quad (7)$$

$$F_i^{\text{conv}} = \chi_{ij} \frac{\partial s}{\partial x_j}. \quad (8)$$

Note the last term in Equation 7, which is proportional to the rotation rate itself rather than its derivatives. With this term (" $\Lambda$  effect") present (and non-zero) in the Reynolds stress, rigid rotation is no longer stress free. The first term on the right hand side of Eq. 7 is the turbulence viscosity, which is generally anisotropic in a rotating stratified convection zone. The same holds for the turbulent heat diffusion coefficient  $\chi_{ij}$  in Eq. 8. The latter anisotropy has a profound impact on the dynamics of the convection zone because it causes the last term on the left hand side of Eq. 6 and thus prevents the cylindrical isocontours predicted by the Taylor Proudman theorem.

Figure .1 shows the internal rotation and meridional flow patterns for the Sun from the mean field model. The differential rotation is in very good agreement with those found by helioseismology. Isocontours are nearly radial at low latitudes while a more disk-shaped pattern is found at the polar caps. At the surface the equator rotates 30 percent faster than the polar caps. The right picture shows stream lines of the meridional flow. The flow is directed towards the poles at the surface and towards the equator at the bottom of the convection zone. Note that the stagnation point is close to the bottom and the return flow thus confined to a shallow layer at the lower boundary. This results in flow speeds about half as high at the surface, despite a density contrast much larger than a factor of two. This flow pattern is in line with the flux transport dynamo, which requires a large-scale counterclockwise flow to reproduce the butterfly diagram of sunspots.

### 3. Reynolds stress versus baroclinic flow

There are two competing mechanisms that drive differential rotation, namely the  $\Lambda$  effect and the meridional flow. The latter, however, can be the result of differential rotation as well as its cause. To illustrate the effect of the baroclinic term in Eq. 4, we compute a model where this term has been switched off. Figure .2 shows the resulting rotation and flow patterns. The rotation pattern is more cylindrical than in the full model and the overall differential rotation is much weaker. This is because the differential rotation term  $\partial \Omega^2 / \partial z$

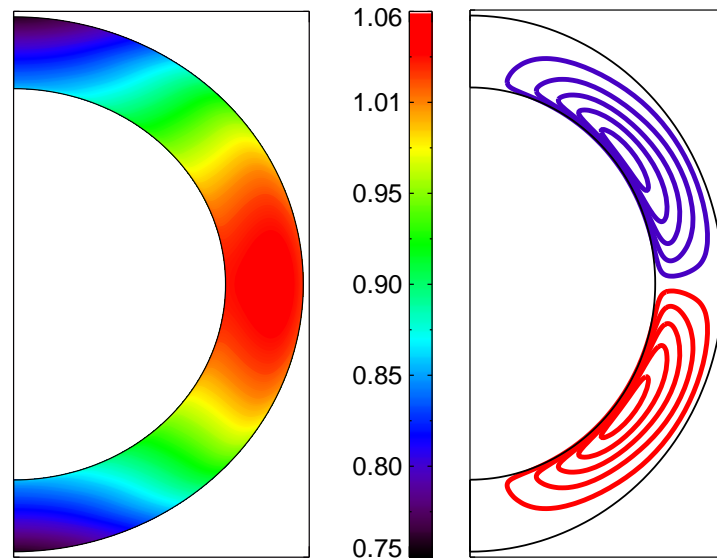


Figure .1: Rotation rate (left) and meridional flow (right) from the full mean field model. In the right diagram, blue lines mean counter-clockwise flow, red lines clockwise.

has to be balanced by the Reynolds stress alone, which for large Taylor number can only be fulfilled if the isocontours of the rotation rate are near-cylindrical. Note that flow speed and pattern are similar to the full model. Note that a meridional flow driven by differential rotation alone will always act against it, i.e. reduce the shear.

We now explore the importance of the  $\Lambda$  term in the Reynolds stress by computing a model where this term has been switched off and the differential rotation is caused solely by the meridional flow. Figure .3 shows the resulting rotation and flow patterns. The surface differential rotation is very similar to the full model. The internal rotation pattern, however, shows disk-shaped rather than radial isocontours. The meridional flow pattern, however, is drastically changed. While there is still one flow cell per hemisphere, the flow direction is now reverse, i.e. towards the equator at the surface and towards the poles at the bottom of the convection zone. Moreover, the surface flow is slower than the flow at the bottom of the convection zone.

As our examples show, the two driving terms in Eq. 4 oppose each other. Solar-type differential rotation drives a counter-clockwise flow, while the baroclinic term caused by a slight increase of the temperature towards the poles drives a flow in the opposite direction. In the full model, the effect of the differential rotation is stronger and the flow is counter-clockwise. The baroclinic term is nonetheless vital as it prevents the differential from being smoothed out by the flow.

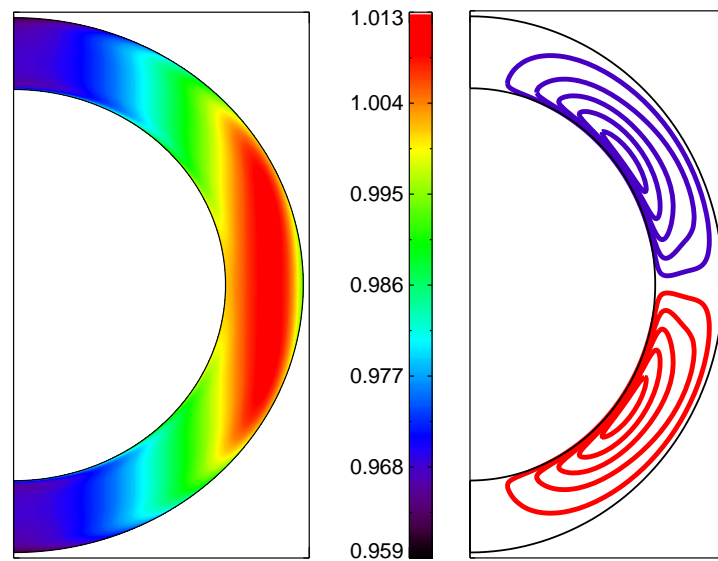


Figure .2: Rotation rate (left) and meridional flow (right) from a model where the baroclinic term has been switched off and the differential rotation is the sole driver of the meridional flow.

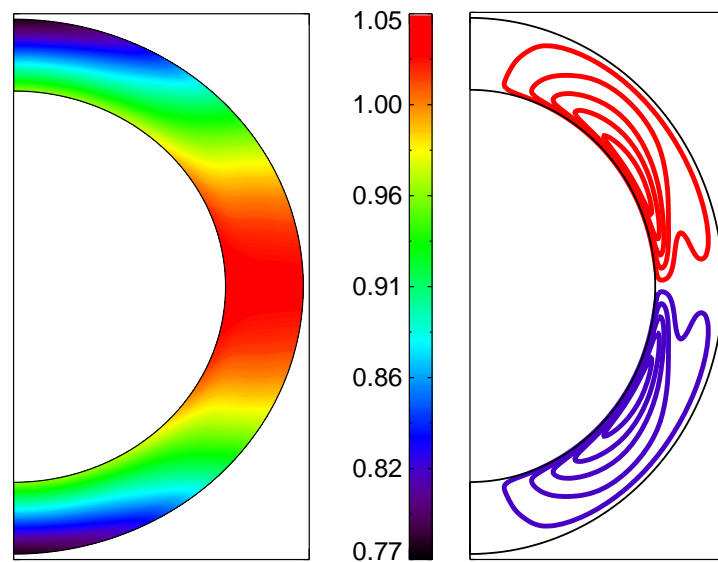


Figure .3: Rotation rate (left) and meridional flow (right) from a model where the baroclinicity is the sole driver of the meridional flow and the Reynolds stress is purely diffusive.

#### 4. Conclusions

Mean field models that combine non-diffusive Reynolds stress and anisotropic helicity transport reproduce both the solar differential rotation and the surface meridional flow. Models based on a baroclinic flow alone can reproduce the surface rotation law but the internal rotation pattern differs substantially from the one observed by helioseismology. Moreover, these models produce a meridional flow pattern that not only contradicts the results from helioseismology, but also the assumptions underlying the flux transport dynamo. The latter requires a counter-clockwise flow (in the northern hemisphere) to reproduce the solar butterfly diagram.

*Acknowledgements.* Thanks to the organizers of Cools Stars 18 for a great meeting.

#### References

- Choudhuri, A.R., Schüssler, M., Dikpati, M. 1995, A&A, 303, 29
- Komm, R., González Hernández, I, Hill F, et al. 2013, Solar Phys, 287, 85
- Küker, M., Rüdiger, G., Kitchatinov, L.L. 2011, A&A 530, 48
- Rüdiger, G., Brandenburg, A. 1995, A&A, 296, 557
- Thompson, M.J., Christensen-Dasgaard, J., Miesch, M.S., Toomre, J. 2003, Annu. Rev. Astron. Astrophys., 2003.41, 599